

UDC 553.4(574)
IRSTI 26.23.13

<https://doi.org/10.55452/1998-6688-2025-22-3-356-369>

^{1*}**Tulepbayev K.,**

Master, ORCID ID: 0009-0006-4384-4483,

*e-mail: k_tulepbayev@kbtu.kz

¹**Tulemissova Zh.,**

PhD, Associate Professor, School of Geology, ORCID ID: 0000-0003-1803-4535,

e-mail: z.tulemissova@kbtu.kz

¹Kazakh-British Technical University, Almaty, Kazakhstan

HYDROTHERMAL ALTERATION AND MINERALOGICAL ZONATION AT THE BOZSHAKOL PORPHYRY COPPER DEPOSIT: INTEGRATION OF SPECTRAL, MAGNETIC, AND 3D MODELING DATA

Abstract

This study investigates the mineralogical and spatial characteristics of hydrothermal alteration at the Bozshakol porphyry copper deposit within the Central Asian Orogenic Belt (CAOB) in Kazakhstan. Geological and geophysical exploration conducted from 2018 to 2024 provided an extensive dataset comprising approximately 24,000 meters of drill core samples collected at two-meter intervals. Analytical methods included short-wave infrared (SWIR) spectroscopy using Arcspectro FT-NIR Rocket (900–2600 nm) and TerraSpec4 spectrometer (350–2500 nm), complemented by magnetic susceptibility measurements utilizing a KT-10 kappameter. Spectral data interpretation employed The Spectral Geologist (TSG) software, integrating automated mineral identification (TSA algorithm) and manual validation (Aux Match). This integrated approach precisely mapped hydrothermal alteration zones, delineating potassic, phyllic, and propylitic facies, each defined by distinct mineral assemblages and magnetic signatures. Potassic alteration, located centrally, features secondary biotite and K-feldspar. This transitions outward into a phyllic halo characterized by pervasive sericitization and reduced magnetite content. The peripheral propylitic zone displays abundant chlorite, epidote, carbonate minerals, and elevated magnetic susceptibility due to magnetite preservation. A key outcome was identifying zones rich in chlorite and epidote, known to adversely affect flotation recovery rates, thus impacting ore-processing efficiency. Leapfrog Geo software facilitated 3D modeling, enhancing visualization and structural interpretation of alteration domains. This comprehensive characterization significantly improves geological understanding and supports optimized exploration and processing strategies, demonstrating best practices in applying modern spectroscopic and geophysical methods to porphyry copper deposits.

Keywords: Bozshakol deposit, porphyry copper systems, hydrothermal alteration, mineral zonation, potassic alteration, phyllic alteration, propylitic alteration, infrared spectroscopy.

Introduction

Porphyry copper deposits represent one of the most economically significant types of ore deposits globally due to their extensive scale, high metal grades, and valuable by-products such as molybdenum, gold, and silver. These deposits are critical resources underpinning modern technological societies, playing a central role in supplying metals essential for infrastructure development, electronics, renewable energy systems, and various industrial applications. The economic viability and longevity of mining operations in these deposits rely significantly on understanding their geological and mineralogical characteristics, especially the hydrothermal alteration zonation.

Hydrothermal alteration in porphyry copper deposits typically manifests as distinct concentric zones surrounding magmatic intrusions [1]. The primary alteration types include potassic, propylitic, phyllic, and argillic, each characterized by unique mineralogical assemblages and distinct metal associations [2]. Potassic zones, typically located near the intrusion cores, commonly exhibit higher concentrations of copper and molybdenum, making them prime exploration and mining targets.

Conversely, propylitic alteration typically marks the peripheral margins of the mineralizing system, usually containing lower metal grades. Intermediate phyllic zones, dominated by sericite, often indicate transitional hydrothermal conditions and are crucial in exploring deeper, economically promising mineralization. Recognizing and accurately mapping these alteration zones is not only vital for exploration and resource estimation but also crucial for optimizing metallurgical processes. Certain minerals, notably chlorite, epidote, and various clay minerals, can adversely affect ore processing methods, particularly flotation efficiency, underscoring the economic importance of precise alteration characterization.

Globally, major porphyry copper systems such as Bingham Canyon (USA), Chuquibambilla (Chile), and Oyu Tolgoi (Mongolia) have been extensively studied, providing robust models of alteration zonation and fluid evolution [2]. Despite significant advancements in understanding these systems, regional variations due to geological, structural, and tectonic differences remain poorly defined in many other deposits.

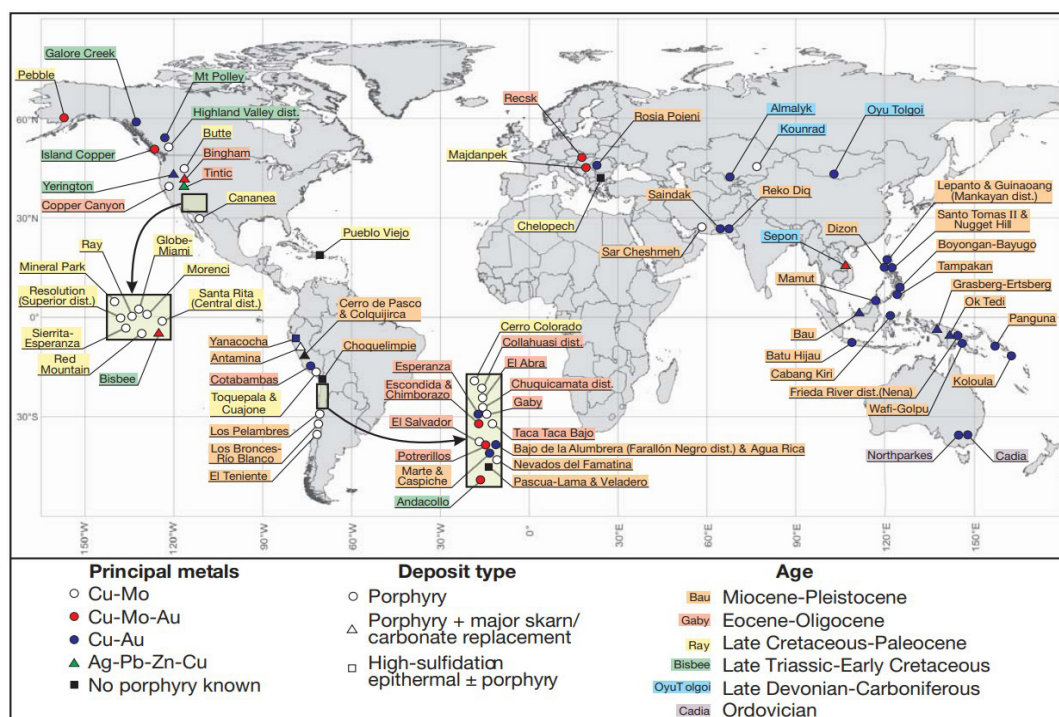


Figure 1 – Global map of the location, age, deposit type and principal metals of major porphyry copper deposits (Sillitoe, 2010)

Kazakhstan hosts several world-class porphyry copper deposits, including Bozshakol, Kounrad, and Aktogay, with Bozshakol standing out due to its large scale and strategic importance. Located within the Kipchak Paleozoic island arc volcanic belt, part of the expansive Central Asian Orogenic Belt (CAOB), Bozshakol provides a unique geological setting to study porphyry copper mineralization formed under Paleozoic subduction-related tectonics [3]. Previous geological studies conducted at Bozshakol laid foundational understanding of its geological structure and broad alteration patterns. However, these earlier works predominantly employed traditional geological methods, providing limited spatial resolution and often insufficient mineralogical detail for modern exploration and processing requirements.

Recent developments in analytical methodologies have significantly improved the capacity to accurately identify and map hydrothermal alteration minerals. Infrared spectroscopy, in particular, has emerged as a highly effective technique for rapid and precise mineral identification in geological materials. When combined with magnetic susceptibility measurements and advanced three-

dimensional modeling techniques, these methods offer unparalleled accuracy and spatial resolution in defining alteration zones and their economic implications.

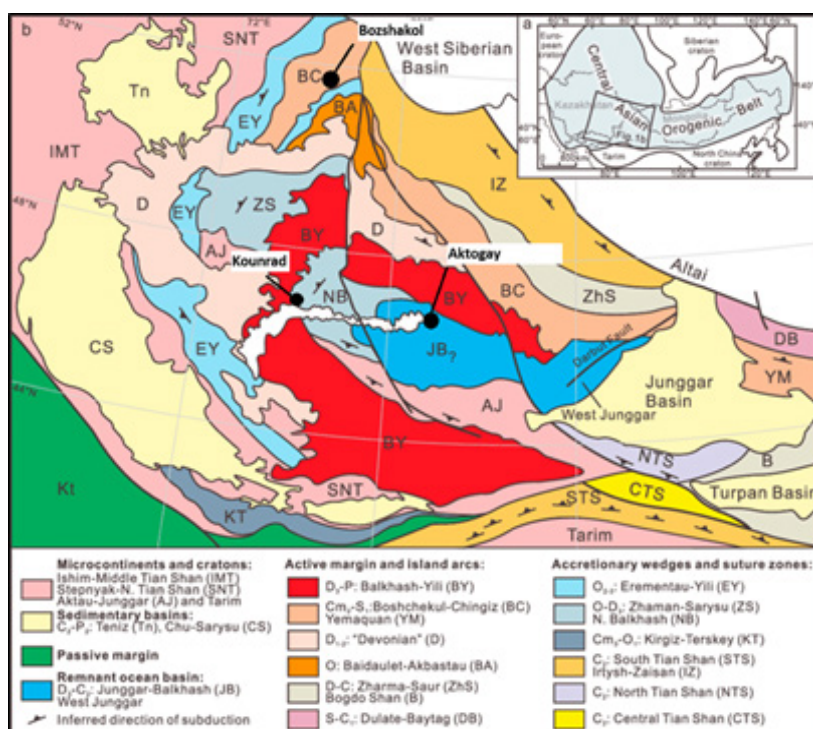


Figure 2 – Simplified regional geological map clearly illustrating the Central Asian Orogenic Belt (CAOB)

Given this technological advancement and the geological potential of Bozshakol, the current study aims to address existing knowledge gaps by deploying state-of-the-art spectroscopic techniques and integrating multiple analytical datasets into detailed three-dimensional geological models. Specifically, this research seeks to: (1) delineate the mineralogical types and spatial zonation of hydrothermal-metasomatic alterations at the Bozshakol deposit, (2) identify and characterize alteration minerals that negatively affect copper recovery efficiency, and (3) establish robust criteria for improved exploration targeting and ore-processing strategies.

Ultimately, the outcomes of this research are expected to significantly enhance geological understanding, improve resource management efficiency, and provide a valuable methodological framework applicable to similar porphyry systems worldwide.

Materials and methods

The present study is based on an extensive collection of drill core samples retrieved from exploration boreholes across the Bozshakol deposit between 2018 and 2024. The total volume of analyzed core reaches approximately 24,000 meters, with systematic sampling conducted every 2 meters. This regular interval was chosen to ensure comprehensive spatial coverage across all lithological domains and alteration zones. Each sample, typically between 2 and 5 cm in length, was prepared by careful washing with distilled water, drying under controlled laboratory conditions, labeling, and individual packaging to prevent contamination. Drill holes were selected based on their spatial coverage across the main ore body and peripheral zones, ensuring representation of all known alteration types.

Infrared spectroscopy (IR spectroscopy) is a powerful analytical technique extensively utilized in geology for identifying and characterizing minerals based on their molecular structures. The

method involves directing infrared radiation onto a geological sample and measuring the absorption of energy at SWIR wavelengths, which correspond to vibrations of chemical bonds within minerals. Each mineral has distinct absorption patterns or “fingerprints” arising from vibrations of molecular bonds, such as stretching or bending of hydroxyl groups, carbonate groups, silicates, and other functional groups. These characteristic absorption bands allow geologists to rapidly and accurately identify mineral phases, even in complex mixtures [4].

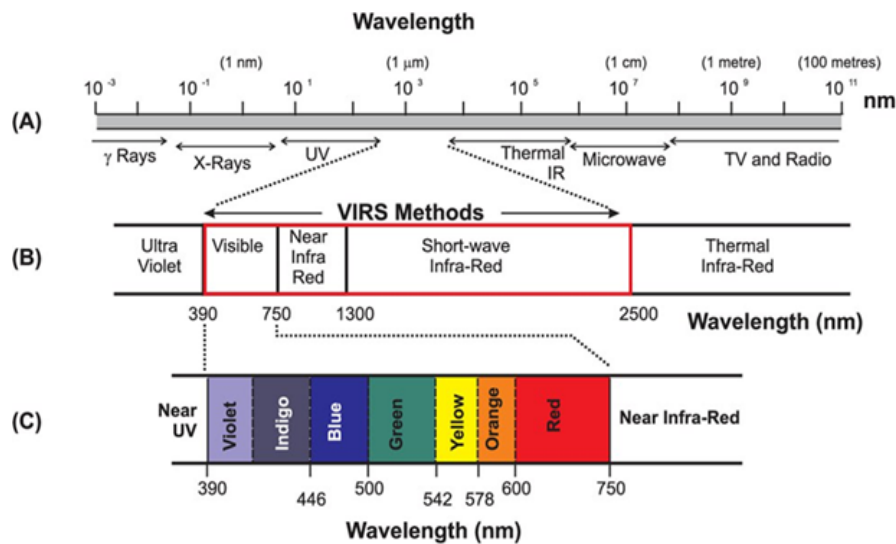


Figure 3 – Distribution of electromagnetic waves along wavelengths

Modern Fourier-transform infrared (FTIR) spectroscopy enhances precision by simultaneously acquiring absorption data across a broad spectral range, enabling detailed analysis of subtle mineralogical variations. Geological samples, including drill core, rock chips, or powders, are commonly analyzed via techniques like transmission, diffuse reflectance, or attenuated total reflectance (ATR).

Type	Silicate structure	Mineral group	Example	VNIR response	SWIR response	LWIR response
Silicates	Inosilicates	Amphibole	Actinolite	Non-diagnostic	Good	Moderate
		Pyroxene	Diopside	Good	Moderate	Good
	Cyclosilicates	Tourmaline	Elbaite	Non-diagnostic	Good	Moderate
	Nesosilicates	Garnet	Grossular	Moderate	Non-diagnostic	Good
		Olivine	Forsterite	Good	Non-diagnostic	Good
	Sorosilicates	Epidote	Epidote	Non-diagnostic	Good	Moderate
	Phyllosilicates	Mica	Muscovite	Non-diagnostic	Good	Moderate
		Chlorite	Clinocllore	Non-diagnostic	Good	Moderate
		Clay minerals	Illite	Non-diagnostic	Good	Moderate
			Kaolinite	Non-diagnostic	Good	Moderate
	Tectosilicates	Feldspar	Orthoclase	Non-diagnostic	Non-diagnostic	Good
			Albite	Non-diagnostic	Non-diagnostic	Good
		Silica	Quartz	Non-diagnostic	Non-diagnostic	Good
Non-silicates	Carbonates	Calcite	Calcite	Non-diagnostic	Moderate	Good
		Dolomite	Dolomite	Non-diagnostic	Moderate	Good
	Hydroxides	Gibbsite	Gibbsite	Non-diagnostic	Good	Moderate
		Alunite	Alunite	Moderate	Good	Moderate
	Sulphates	Gypsum	Gypsum	Non-diagnostic	Good	Good
		Borates	Borax	Non-diagnostic	Moderate	TBD
	Halides	Chlorides	Halite	Non-diagnostic	TBD	TBD
	Phosphates	Apatite	Apatite	Moderate	Non-diagnostic	Good
	Hydrocarbons		Bitumen	TBD	Moderate	TBD
	Oxides	Hematite	Hematite	Good	Non-diagnostic	Non-diagnostic
		Spinel	Chromite	Non-diagnostic	Non-diagnostic	Non-diagnostic
	Sulphides		Pyrite	Non-diagnostic	Non-diagnostic	Non-diagnostic

Figure 4 – Qualitative accuracy of spectral analyses in VNIR, SWIR, and LWIR ranges

IR spectroscopy is particularly effective for studying clay minerals, chlorite, epidote, carbonates, sulfates, and other alteration minerals commonly associated with hydrothermal systems. By identifying these minerals, geologists can reconstruct hydrothermal alteration patterns, interpret geological history, assess economic mineralization potential, and determine ore-processing characteristics, notably flotation performance. Thus, infrared spectroscopy plays a critical role in mineral exploration, deposit modeling, and geometallurgical assessments in geological research.

Two infrared spectrometers were used over the multi-year program [9]. From 2018 to 2020, analyses were performed with a Fourier-transform spectrometer Arcspectro FT-NIR Rocket equipped with an ArcSphere-50-Hal integrating sphere. This configuration allowed SWIR spectra to be collected across the 900–2600 nm range. The Arcspectro system was calibrated using a suite of mineral standards before each analytical session to ensure spectral accuracy.

A quality assurance and quality control (QA/QC) protocol was implemented during sample collection and preparation. Duplicate measurements, white reference was regularly used to assess consistency. Data verification included statistical validation of mineralogical trends and cross-comparison between spectroscopic outputs and geological logs.

Beginning in 2021, a TerraSpec4 portable spectrometer with improved detection capacity (350–2500 nm range) was employed for all new core analyses. Calibration of the TerraSpec4 was conducted daily using a white reference panel (Spectralon) and dark current correction. The enhanced spectral resolution and stability of the TerraSpec4 allowed for the identification of subtle mineralogical features, including variations within white mica and chlorite groups.

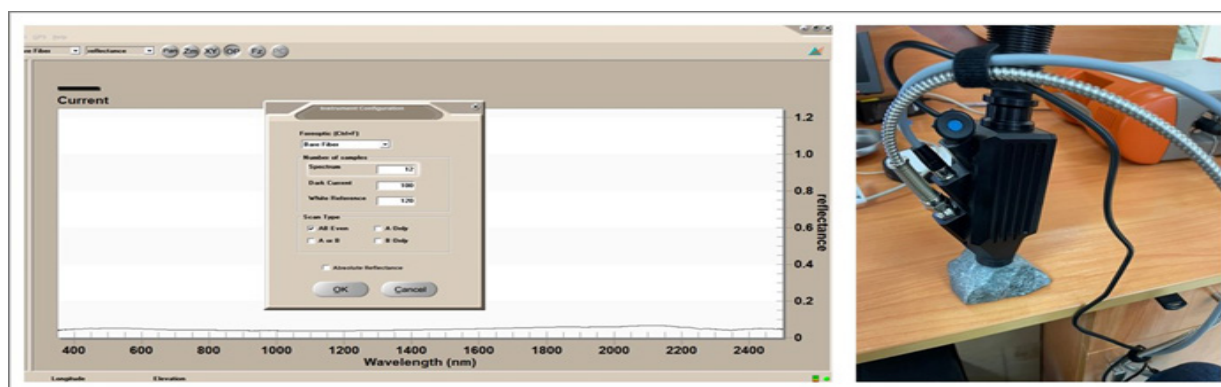


Figure 5 – Sample preparation and spectral analysis using TerraSpec4 instrument

Spectral data were interpreted using The Spectral Geologist 8 (TSG) software, which integrates two primary analytical tools: The Spectral Assistant (TSA) for automated mineral recognition based on established libraries, and Aux Match, a comparative tool allowing alignment of unknown spectra with known reference patterns. The TSA algorithm uses continuum removal, derivative analysis, and a similarity index to match unknowns to diagnostic minerals. Aux Match functions as a visual overlay tool to refine identifications when multiple species are spectrally similar. Outputs included mineral group classification, confidence levels, and spatial variation trends.

The Spectral Geologist (TSG) software version 8 is a powerful tool for interpreting spectral data obtained with a spectrometer.

The interpretation of spectra using TSG-8 is carried out in the following sequence:

- ♦ Data loading: First, spectral data is loaded into TSG-8. This can be data obtained directly from the instrument or imported from other sources.
- ♦ Preprocessing: The software performs data preprocessing, including background correction and noise removal, to improve the quality of spectral signals.
- ♦ Mineral identification: TSG-8 uses a library of reference spectra to match measured spectra with known minerals. The software determines the presence and concentration of minerals in the sample.

- ♦ Quantification: The software allows for quantitative analysis by estimating the percentage of each mineral in the sample.
- ♦ Visualization: TSG-8 provides various tools for data visualization, including mineral distribution maps, histograms, and 3D models.
- ♦ Reporting: The software creates reports and graphs that demonstrate the results of the analysis, then the report is downloaded in text format with all the information on the mineral composition of the samples for further inclusion in the database.

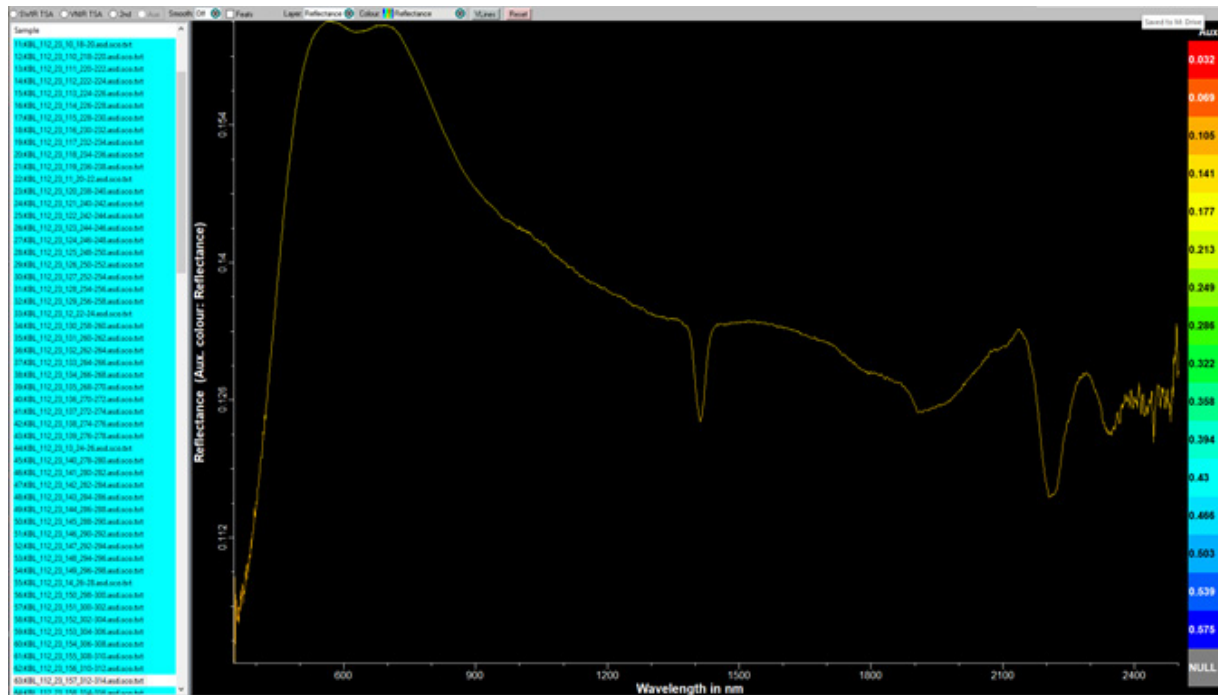


Figure 6 – Example of graphical reports on the mineral composition of a sample in TSG-8:
(a) Reflectance spectrum curve of the sample;
(b) Quantitative summary of the constructed mineral database of borehole

Hole_ID	From	To	Sample_ID	Min1_sTAS	Wt1_sTAS	Min2_sTAS	Wt2_sTAS	Min3_sTAS	Wt3_sTAS	w2200	d2200	Kaolinite_Cry	Sericite_Cry	w2250	d2250	w2350	d2350	d1900	smectite
KBL_010_21	22	24	12	Chlorite-Fe	0.574	Montmorillonite	0.426				0.00358			0.138	2238.28	0.0127	2353.68	0.026	0.426
KBL_010_21	24	26	13	Kaolinite-WX	0.556	Montmorillonite	0.444			2207.49	0.018	1.988	0.708		0.00328	2360.48	0.00452	0.0255	0.444
KBL_010_21	26	28	14	Kaolinite-PX	0.547	Chlorite-Fe	0.453			2207.41	0.0286	2.462	1.072	0.245	0.00879	2347.62	0.00287	0.0267	
KBL_010_21	28	30	15	Montmorillonite	0.4	Epidote	0.359	Kaolinite-WX	0.24	2207.83	0.0201		0.832	2252.36	0.0187	2338.64	0.0161	0.0242	0.7
KBL_010_21	30	32	16	Chlorite-FeMg	0.542	Phengiticillite	0.458				0.0158	1.064	2246.3	0.014	2343.41	0.00525	0.0149	0.4	
KBL_010_21	32	34	17	Chlorite-FeMg	0.711	Montmorillonite	0.289						2253.47	0.00596	2338.03	0.00274	0.00543	0.289	
KBL_010_21	34	36	18	Kaolinite-WX	0.404	Montmorillonite	0.306	Chlorite-FeMg	0.29	2207.86	0.0273	2.41	1.221	2248.12	0.00791	2352.8	0.00395	0.0223	0.306
KBL_010_21	36	38	19	Montmorillonite	0.372	Chlorite-FeMg	0.354	Kaolinite-WX	0.274	2208.22	0.0146		1.401	2249.11	0.00807	2355.52	0.00303	0.0104	0.372
KBL_010_21	38	40	20	Chlorite-Fe	0.531	Montmorillonite	0.469			2208.41	0.0112		0.477	2246.9	0.0109	2349.71	0.00235	0.469	
KBL_010_21	40	42	21	Montmorillonite	0.464	Chlorite-Fe	0.32	Kaolinite-PX	0.216	2205.98	0.028		0.911	2242.28	0.011	2352.86	0.00367	0.0308	0.464
KBL_010_21	42	44	22	Chlorite-Fe	0.398	Siderite	0.37	Muscovite	0.232	2209.07	0.0048		0.842	2252.35	0.00438	2333.9	0.00313	0.0057	
KBL_010_21	44	46	23	Chlorite-FeMg	0.504	Montmorillonite	0.496			2214.19	0.00229		0.295	2249.65	0.00255	2343.13	0.00218	0.00776	0.496
KBL_010_21	46	48	24	Muscovite	0.618	Magnetite	0.382			2207.08	0.00651		0.184	2249.37	0.00381	2344.12	0.00243	0.0353	
KBL_010_21	48	50	25	Chlorite-FeMg	0.5	Muscovite	0.5			2205.63	0.0039		2.56		0.00636	2344.11	0.00498	0.0133	
KBL_010_21	50	52	26	Muscovite	1					2206.76				2233.39		2344.49	0.00206	0.0107	
KBL_010_21	52	54	27	Chlorite-FeMg	0.796	Kaolinite-PX	0.204			2208.37	0.0166		0.962	2250.48	0.0257	2340.63	0.00723	0.0172	
KBL_010_21	54	56	28	Montmorillonite	0.571	Chlorite-Fe	0.429			2209.21	0.0126		0.37	2232.34	0.0172	2356.31	0.00315	0.0341	0.571
KBL_010_21	56	58	29	Asphat	1					2214.06				2253.35		2328.94		0.00224	
KBL_010_21	58	60	30	Chlorite-FeMg	1					2224.86				2249.55	0.00188	2327.75	0.0026		
KBL_010_21	60	62	31	Montmorillonite	0.616	Chlorite-FeMg	0.384			2218.63	0.00952		0.268	2243.75	0.0181	2340.17	0.00362	0.0356	0.616
KBL_010_21	62	64	32	Phengite	0.403	Chlorite-Fe	0.385	Magnetite	0.212	2221.15	0.00319		0.47	2250.96	0.00413	2343.44	0.0066		
KBL_010_21	64	66	33	Muscoviticillite	0.509	Chlorite-FeMg	0.495			2219.26	0.00278		0.339	2230.7		2340.74	0.00516		
KBL_010_21	66	68	34	Montmorillonite	1					2221.83						2335.84	0.00468	1	
KBL_010_21	68	70	35	Chlorite-FeMg	0.616	Muscovite	0.384			2216.84				2252.69	0.00283	2332.67	0.00368		
KBL_010_21	70	72	36	Chlorite-FeMg	0.784	Phengiticillite	0.216			2221.23	0.00308		0.388	2252.8	0.00736	2343.02	0.00325	0.00793	
KBL_010_21	72	74	37	Siderite	0.56	Montmorillonite	0.44			2215.91				2230.63		2325.41		0.44	
KBL_010_21	74	76	38	Muscoviticillite	0.574	Chlorite-FeMg	0.426			2219.96	0.0146		0.832		0.00721	2340.67	0.00414	0.0175	
KBL_010_21	76	78	39	Chlorite-Mg	0.553	Montmorillonite	0.447			2209.87	0.00293	3.326	0.661	2249.26		2332.94	0.00444	0.447	
KBL_010_21	78	80	40	Montmorillonite	0.431	Chlorite-FeMg	0.325	Calcite	0.243	2209.39		2.423		2247.79	0.00332	2336.12	0.00505	0.0137	0.431
KBL_010_21	80	82	41	Chlorite-FeMg	0.713	Muscoviticillite	0.287			2223.28	0.00196			2251.05	0.00273	2341.13	0.00279		
KBL_010_21	82	84	42	Montmorillonite	0.636	Chlorite-FeMg	0.364			2208.59	0.00269		0.146			2342.95	0.00244	0.0183	0.636
KBL_010_21	84	86	43	Chlorite-FeMg	0.564	Montmorillonite	0.436			2221.31				2248.95	0.00541	2338.19	0.00307	0.00311	0.436
KBL_010_21	86	88	44	Asphat	1					2215.23				2229.6		2323.96			
KBL_010_21	88	90	45	Muscovite	0.706	Chlorite-Mg	0.294			2205.86	0.00475			2233.37		2342.7	0.00194		
KBL_010_21	90	92	46	Phengiticillite	0.55	Chlorite-FeMg	0.45			2215.69	0.00549		2.396		0.00455	2340.64	0.0037	0.00229	
KBL_010_21	92	94	47	Phengiticillite	0.817	Chlorite-Mg	0.183			2213.47	0.00567		1.916			2336.82	0.0104	0.00387	
KBL_010_21	94	96	48	Chlorite-FeMg	0.571	Calcite	0.221	Montmorillonite	0.208	2221.63	0.00204		0.296	2250.76	0.0107	2333.12	0.00538	0.00608	0.208
KBL_010_21	96	98	49	Chlorite-FeMg	1									2250.93	0.00377	2324.99	0.00256	0.00349	

Figure 7 – Preparation of a spectral database for 3D modeling

Spectral data were exported in .csv format and aligned with corresponding sample depths, lithological units, and logging metadata. These results were used to generate vertical mineralogical profiles and cross-sectional interpretation panels. Where possible, spectral interpretations were validated by petrographic observations.



Figure 8 – Handheld KT-10 kappameter

In parallel, magnetic susceptibility was measured using a handheld KT-10 kappameter with a 10 kHz coil frequency and 2.5 cm penetration depth, with interpretation guided by established magnetic properties of hydrothermal mineral assemblages [7]. Each 2-meter interval was measured three times on fresh, unfractured core surfaces, and values were averaged to minimize variability. Calibration was conducted using a zero-reference block and high-susceptibility magnetite standard. Reproducibility tests indicated an average relative standard deviation below 3%.

Susceptibility data were analyzed in conjunction with lithology and alteration intensity to delineate magnetite-bearing propylitic zones and distinguish weakly magnetic phyllic zones. Threshold values for susceptibility were established based on population statistics and confirmed through spatial comparison with mineralogical observations.

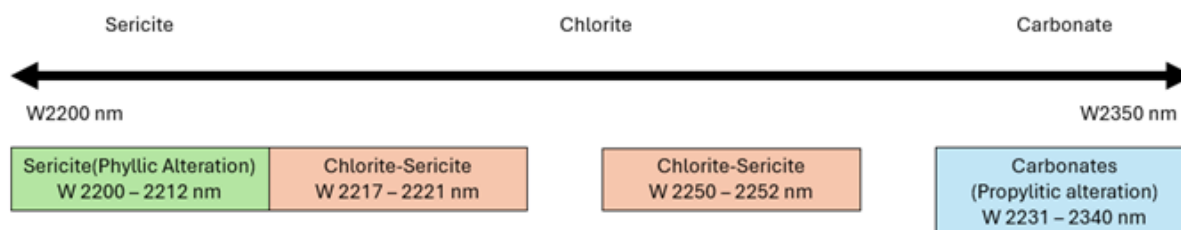


Figure 9 – Numerical Models derived from identified earlier alteration zones

Spectral signatures used in the data analysis:

- ♦ Muscovite: The distinctive spectral characteristics of muscovite (sericite) are found in the wavelength range from 2200 to 2210 nm, designated w2200.
- ♦ Phengite: Sericite alteration associated with phengite is identified by the spectral wavelength of 2210 nm.
- ♦ Chlorite: Information about the magnesium or iron content of chlorite is revealed by absorption signatures in the range between 2240 and 2268 nm.
- ♦ Carbonates and mafic minerals: The spectral signature at 2350 nm is characteristic of carbonate minerals and indicates the presence of absorption due to vibrational movements of CO₃ molecules. This indicator is often well expressed and easily detected in spectral measurements.

Numerous numerical models were built in Leapfrog software (“reference” models) in the indicated ranges of values.

For the previously identified types of hydrothermal-metasomatic alterations, the following numerical models were selected:

- ♦ Sericitic (Phyllic) – Digital model w2200 range 2200–2212 nm.
- ♦ Chlorite-sericite – Digital model w2200 range 2217–2221 nm and model w2250 range 2250–2252 nm.
- ♦ Propylitic (Chlorite-epidote-albite-carbonate) – Digital model w2200 range 2212–2214 nm and model w2350 range 2331–2340 nm

The “baseline” numerical models provided a basic understanding of the distribution of alteration zones at Bozshakol, allowing for a more in-depth interpretation of the data.

Results and discussion

Detailed spectral analysis, integrated with magnetic susceptibility measurements and geological logging, provided comprehensive insights into the hydrothermal alteration zoning at the Bozshakol deposit. Three distinct alteration zones—potassic, phyllic, and propylitic—were identified, each demonstrating unique mineralogical characteristics corresponding to classical copper porphyry alteration zoning [1].

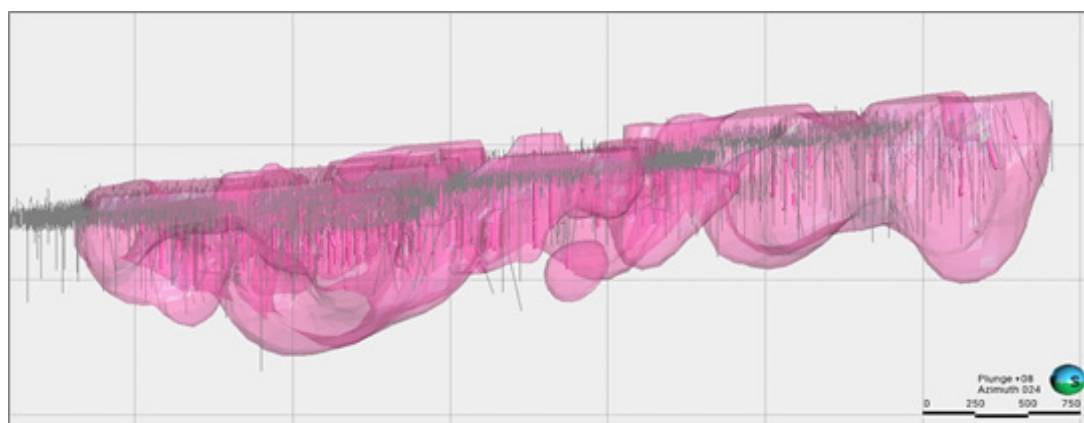


Figure 10 – Distribution of the potassic alteration zone, with labeled spectral features

The potassic alteration zone was primarily observed in central and deeper regions of the deposit [8]. This zone exhibited a pronounced dominance of secondary biotite and K-feldspar, confirmed through consistent infrared spectral signatures, including diagnostic absorption peaks around 2350 nm (Mg-OH bonds) for biotite and around 2200 nm (Al-OH bonds) for K-feldspar. Potassic alteration zones consistently yielded moderate magnetic susceptibility values (approximately $3\text{--}6 \times 10^{-3}$ SI units), correlating with variable magnetite content resulting from hydrothermal processes. The presence of secondary biotite and K-feldspar in this zone indicates the highest-temperature alteration conditions associated with mineralizing fluids at Bozshakol.

Surrounding the potassic core, the phyllic alteration zone was characterized by widespread sericitization, predominantly expressed as fine-grained sericite (muscovite). Spectral features diagnostic of sericite were frequently noted around 2200 nm, with variations towards shorter wavelengths (approximately 2195 nm) reflecting Al-rich muscovite compositions. Magnetic susceptibility in the phyllic alteration zone was notably low, typically below 2×10^{-3} SI units, indicative of significant destruction or alteration of magnetite due to intense hydrolytic processes. The well-

defined spatial extent and mineralogical consistency of the phyllic alteration zone suggest extensive fluid-rock interaction under moderately acidic and cooler hydrothermal conditions compared to the central potassic zone.

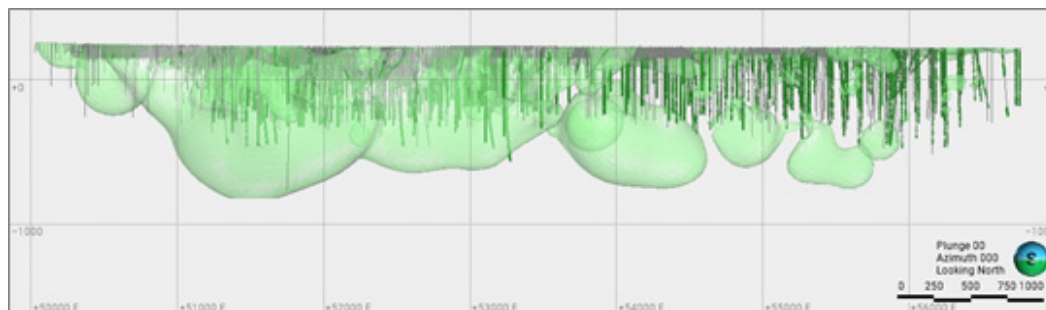


Figure 11 – Numerical model w2200 range 2200-2212nm (sericite)

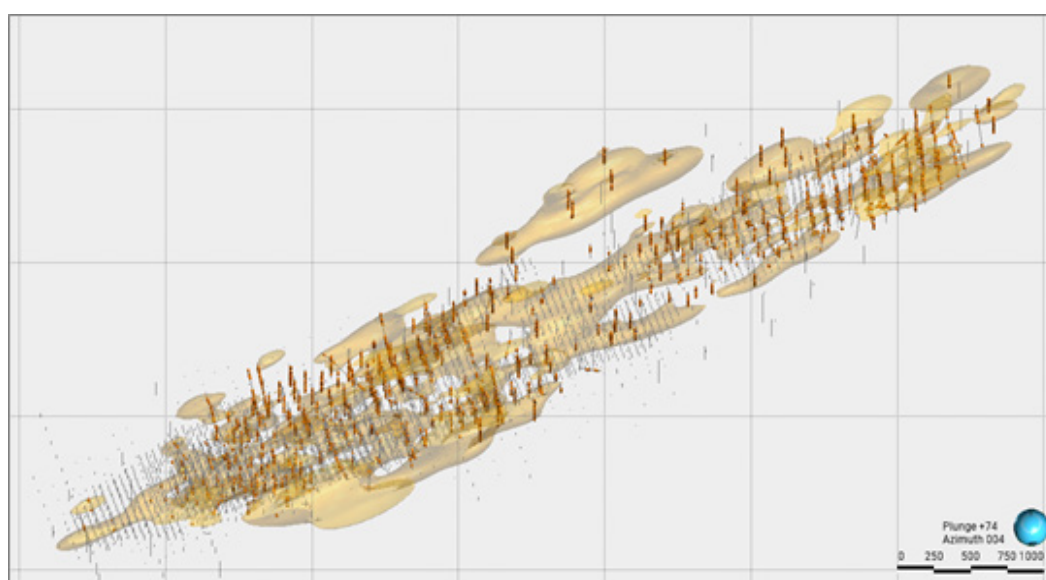


Figure 12 – Numerical model w2250 range 2250-2252nm (chlorite-sericite)

Peripheral to the potassic and phyllic zones, the propylitic alteration exhibited extensive development of chlorite and epidote minerals. Chlorite was frequently identified through characteristic Fe,Mg-OH absorption signatures near 2250 nm and 2340 nm, while epidote showed notable Fe-OH absorption around 1550 nm. High magnetic susceptibility values, frequently exceeding 10×10^{-3} SI units, characterized the propylitic zone due to significant magnetite enrichment, often associated with chlorite. This outermost alteration halo defines the most distal alteration products resulting from relatively low-temperature, neutral to slightly alkaline hydrothermal fluids.

Three-dimensional geological modeling was carried out using Leapfrog Geo 2023.2 software. Logged alteration intervals were manually selected and categorized into alteration types (potassic, phyllic, propylitic) based on spectral data, magnetic response, and visual logging. These intervals were input into the geological model as categorical data using Leapfrog's "interval selection" tool.

Interpolation of alteration zones was conducted using Leapfrog's "Vein Interpolation" and "Lithology Model" modules, applying a boundary-based implicit modeling approach. Interpolations were guided by structural trends and stratigraphic surfaces. Model validation was performed using cross-sections and plan views compared against raw log data, along with volume analysis and overlapping zonal statistics.

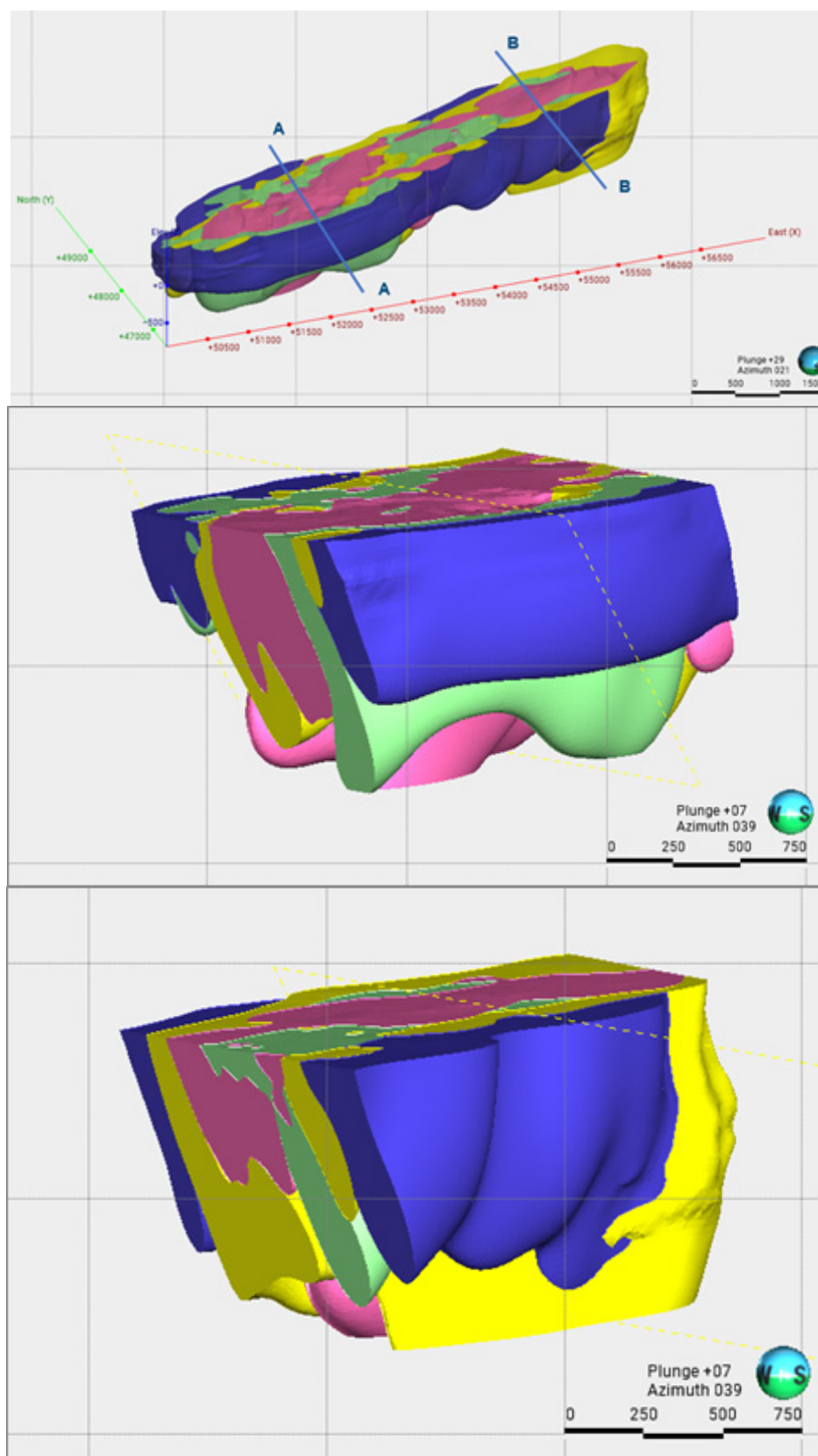


Figure 13 – 3D visualization of alteration zones modeled in Leapfrog Geo 2023.2.
(a) Alteration Model; (b) Section A-A; (c) Section B-B

Together, this multi-technique approach enabled a high-resolution reconstruction of alteration mineralogy and zonation, integrating visual geological observations with advanced analytical datasets. It provided a detailed understanding of the spatial relationships among alteration facies essential for exploration vectoring and process optimization.

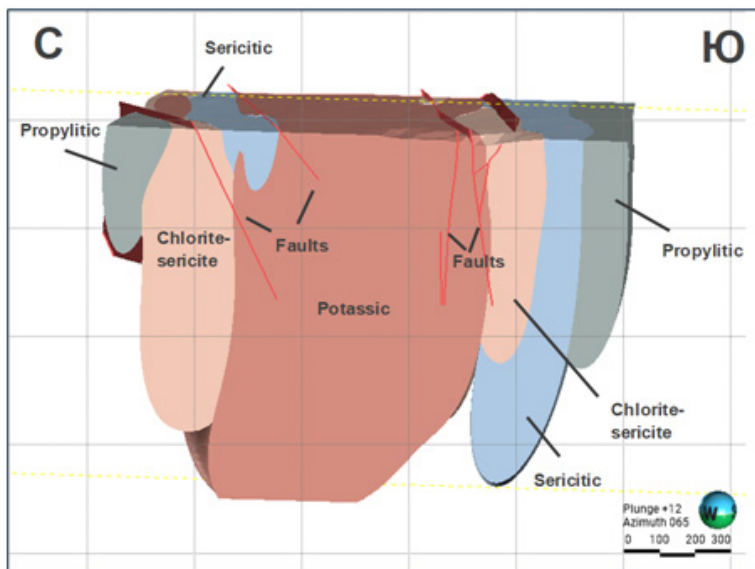


Figure 14 – Extent and characteristics of the alteration zones, clearly labeling areas of chlorite, sericite and epidote enrichment

The identification and spatial characterization of minerals such as chlorite and epidote within the propylitic zone carry significant implications for mineral processing operations. Chlorite, with its platy morphology, often negatively impacts flotation processes by covering sulfide minerals, thus hindering effective reagent adsorption and necessitating increased reagent dosages. Epidote similarly complicates ore processing by increasing pulp viscosity and impeding efficient mineral separation. The clear spatial definition of these minerals enables proactive metallurgical adjustments, optimizing reagent selection, dosing strategies, and pre-treatment processes.

Additional aspects that can be investigated further include the potential influence of host-rock lithology on alteration intensity and mineral distribution, which was suggested by variations observed across different lithological units. Detailed petrographic analyses and mineralogical studies could provide insights into the interactions between hydrothermal fluids and host-rock compositions, potentially refining the interpretation of alteration processes at Bozshakol.

This study also highlighted key analytical limitations. Spectral overlaps, especially between chlorite and epidote, occasionally posed identification challenges despite advanced software solutions provided by TSG's Spectral Assistant (TSA) and Aux Match tools. Future exploration and drilling efforts should emphasize improved interpretation methodologies and additional validation techniques such as X-ray diffraction (XRD) to further mitigate these uncertainties [5].

Future research directions suggested by this study include targeted exploration and drilling efforts, particularly within structurally complex and underrepresented regions. Complementary methods such as detailed geochemical assays, fluid inclusion studies, and stable isotope analyses would provide valuable insights into the temporal evolution of alteration processes, further enhancing the geological model.

In conclusion, the integrated methodological approach applied to the Bozshakol deposit significantly advanced the understanding of its hydrothermal alteration framework. Clearly defined zonation patterns and identified processing implications represent invaluable contributions to both exploration and operational strategies. Furthermore, the methodological insights and outcomes from

this research offer a valuable blueprint for exploring and modeling other complex porphyry copper systems worldwide.

Conclusions

This detailed investigation at the Bozshakol deposit successfully characterized the spatial and mineralogical patterns of hydrothermal alteration through integrated infrared spectral analysis, magnetic susceptibility measurements, and comprehensive geological logging. The research effectively delineated three distinct alteration zones – potassic, phyllic, and propylitic—each marked by unique mineralogical signatures.

The potassic alteration zone was clearly defined by diagnostic minerals such as secondary biotite and K-feldspar, indicating high-temperature hydrothermal processes central to ore formation. This zone's moderate magnetic susceptibility further suggested the complex interplay of magnetite deposition and alteration.

The phyllic alteration zone was characterized by widespread sericite alteration and distinctly low magnetic susceptibility, indicating extensive magnetite destruction due to intense hydrolytic alteration. Clearly defined spectral signatures confirmed the prevalence of Al-rich muscovite compositions, highlighting significant fluid-rock interactions in this intermediate-temperature zone.

Peripheral propylitic alteration, characterized by abundant chlorite and epidote, showed high magnetic susceptibility due to magnetite enrichment. The identification and precise mapping of these minerals hold critical implications for ore processing, especially flotation, where chlorite and epidote notably complicate metallurgical recovery [6].

The practical implications of these findings are substantial, offering clear guidelines for optimized exploration targeting and ore-processing adjustments. Knowledge of specific mineral distributions, particularly of problematic minerals such as chlorite and epidote, enables preemptive metallurgical planning, allowing modifications to reagent usage and treatment strategies to enhance processing efficiency.

This research also identified several analytical limitations and uncertainties, notably spectral overlaps between similar alteration minerals and lack of standardized interpretation of magnetic susceptibility data. Addressing these limitations through development of interpretation methods of magnetic susceptibility and integrating complementary analytical approaches such as X-ray diffraction (XRD) will significantly enhance future studies.

Further research directions recommended by this study include targeted drilling in structurally complex and underrepresented areas, Long-wave infrared (LWIR) spectroscopy, detailed geochemical assays, fluid inclusion analyses, and stable isotope studies. These methodologies promise to deliver deeper insights into alteration processes and the temporal evolution of the hydrothermal system.

Overall, this integrative approach has substantially advanced the geological understanding of the Bozshakol deposit, providing valuable insights directly applicable to exploration and operational strategies. The results of this study serve as a robust methodological framework beneficial for similar porphyry copper deposit investigations worldwide.

REFERENCES

- 1 Lowell, J.D., & Guilbert, J.M. Lateral and vertical alteration-mineralization zoning in porphyry ore deposits. *Economic Geology*, 65(4), 373–408 (1970).
- 2 Sillitoe, R.H. Porphyry Copper Systems. *Economic Geology*, 105(1), 3–41 (2010).
- 3 Yakubchuk, A. Architecture and mineralization of the Central Asian Orogenic Belt and adjacent continental margins. *Tectonophysics*, 351(1-2), 3–31 (2002).
- 4 Clark, R.N. Spectroscopy of rocks and minerals, and principles of spectroscopy. In A.N. Rencz (Ed.), *Remote Sensing for the Earth Sciences: Manual of Remote Sensing*, vol. 3, pp. 3–58 (1999).

- 5 Bish, D.L., & Post, J.E. Modern Powder Diffraction. Reviews in Mineralogy, 20, Mineralogical Society of America (1989).
- 6 Wills, B.A., & Finch, J. Wills' Mineral Processing Technology: An Introduction to the Practical Aspects of Ore Treatment and Mineral Recovery (8th ed.) (Butterworth-Heinemann, Oxford, UK, 2015).
- 7 Hunt, C.P., Moskowitz, B.M., & Banerjee, S.K. Magnetic Properties of Rocks and Minerals. In: Ahrens, T.J. (Ed.), Rock Physics & Phase Relations: A Handbook of Physical Constants. AGU Reference Shelf (American Geophysical Union, 1995), vol. 3, pp. 189–204
- 8 Bekkarnayev, K.S., & Balakov, M.F. Structural-Geological and Alteration Model of the Bozshakol Deposit. Internal Technical Report (2023).
- 9 Professional Geo Solutions LLC. Report on R&D Activities at the Bozshakol Deposit, Kazakhstan. Internal Technical Report (2024).

^{1*}Тулепбаев Қ.,
магистр, 0009-0006-4384-4483,
*e-mail: k_tulepbayev@kbtu.kz
¹Тулемисова Ж.,
PhD, ORCID: 0000-0003-1803-4535,
e-mail: z.tulemissova@kbtu.kz

¹Қазақстан-Британ техникалық университеті, Алматы қ., Қазақстан

БОЗШАКӨЛ МЫС-ПОРФИРЛІ КЕН ОРНЫНДАҒЫ ГИДРОТЕРМИЯЛЫҚ ӨЗГЕРІС ЖӘНЕ МИНЕРАЛОГИЯЛЫҚ АУДАНДАСТЫРУ: СПЕКТРЛІК, МАГНИТТІК ЖӘНЕ 3D МОДЕЛЬДЕУ ДЕРЕКТЕРІН БІРІКТІРУ

Аңдатпа

Бұл зерттеу Қазақстандағы Орталық Азия орогендік белдеуіндегі (ЦАОБ) Бозшакөл порфирлі мыс кен орнындағы гидротермиялық өзгерістердің минералогиялық және кеңістіктік сипаттамаларын қарастырады. 2018 жылдан 2024 жылға дейін жүргізілген геологиялық және геофизикалық барлау жұмыстары шамамен 24 000 метр бұрғылау деректерінен тұратын, екі метрлік аралықпен алынған сынамалар негізінде ауқымды деректер жиынтығын ұсынды. Аналитикалық әдістерге қысқа толқынды инфрақызыл (SWIR) спектроскопиясы қолданылды, атап айтқанда Arcspectro FT-NIR Rocket (900–2600 нм) және TerraSpec4 спектрометрі (350–2500 нм). Бұл әдістер КТ-10 капаметрі арқылы алынған магниттік сезімталдық өлшемдерімен толықтырылды. Спектрлік деректерді интерпретациялау үшін минералдарды автоматтандырылған сәйкестендіру (TSA алгоритмі) және қолмен тексеру (Aux Match) әдістері біріктірілген Spectral Geologist (TSG) бағдарламалық құралы қолданылды. Интеграцияланған тәсіл гидротермиялық өзгеру аймақтарын нақты картаға түсіруге мүмкіндік беріп, калий, филлдік және пропилиттік фацияларды анықтады. Бұл фациялар әрқайсысы ерекше минералдық жинақтармен және магниттік сипаттамалармен ерекшеленеді. Орталық бөлікте орналасқан калийлі альтерация екіншілік биотит пен калийлі дала шпаттарының болуымен сипатталады. Бұл аймақ кең таралған серициттену мен магнетит құрамының төмендеуімен сипатталатын филлдік ореолға ауысады. Шеткі пропилиттік аймақта хлорит, эпидот және карбонат минералдары мол, және магнетиттің сақталуына байланысты жоғары магниттік сезімталдық байқалады. Зерттеудің негізгі нәтижесі – хлорит пен эпидотқа бай аймақтарды анықтау болды. Бұл аймақтар флотация процесіндегі қалпына келу көрсеткіштерін төмендетіп, кенді өңдеу тиімділігіне теріс әсер етеді. Leapfrog Geo бағдарламалық жасақтамасы 3D модельдеуді жеңілдетіп, өзгеру домендерінің құрылымдық интерпретациясы мен визуализациясын жетілдірді. Бұл кешенді сипаттама геологиялық түсінікті едәуір арттырып, порфирлі мыс кен орындарын барлау мен игеруде заманауи спектроскопиялық және геофизикалық әдістерді қолданудың озық тәжірибесін көрсетеді. Сонымен қатар, барлау және өңдеу стратегияларын оңтайландыруға септігін тигізеді.

Тірек сөздер: Бозшакөл кен орны, мыс порфирді жүйелері, гидротермиялық альтерация, минералды аудандастыру, калийлік альтерация, филлиттік альтерация, пропилиттік альтерация, инфрақызыл спектроскопия.

^{1*}Тулепбаев К.,
магистр, ORCID: 0009-0006-4384-4483,
*e-mail: k_tulepbayev@kbtu.kz
¹Тулемисова Ж.,
PhD, ORCID: 0000-0003-1803-4535,
e-mail: z.tulemissova@kbtu.kz

¹Казахстанско-Британский технический университет, г. Алматы, Казахстан

ГИДРОТЕРМАЛЬНЫЕ ИЗМЕНЕНИЯ И МИНЕРАЛОГИЧЕСКАЯ ЗОНАЛЬНОСТЬ НА БОЗШАКОЛЬСКОМ МЕСТОРОЖДЕНИИ МЕДНО-ПОРФИРОВЫХ РУД: ИНТЕГРАЦИЯ СПЕКТРАЛЬНЫХ, МАГНИТНЫХ ДАННЫХ И ДАННЫХ ТРЕХМЕРНОГО МОДЕЛИРОВАНИЯ

Аннотация

В этом исследовании изучаются минералогические и пространственные характеристики гидротермальных изменений на месторождении медно-порфировых руд Бозшаколь в Центрально-Азиатском орогенном поясе (ЦАОП) в Казахстане. Геологическая и геофизическая разведка, проведенная с 2018 по 2024 гг., предоставила обширный набор данных, включающий около 24 000 м образцов кернов, собранных с интервалом в два метра. Аналитические методы включали коротковолновую инфракрасную (SWIR) спектроскопию с использованием Arcspectro FT-NIR Rocket (900–2600 нм) и спектрометра TerraSpec4 (350–2500 нм), дополненную измерениями магнитной восприимчивости с использованием каппаметра КТ-10. Для интерпретации спектральных данных использовалось программное обеспечение The Spectral Geologist (TSG), объединяющее автоматизированную идентификацию минералов (алгоритм TSA) и ручную проверку (Aux Match). Этот комплексный подход точно картировал зоны гидротермальных изменений, очерчивая калиевые, филлитовые и пропилитовые фации, каждая из которых определяется отдельными минеральными ассоциациями и магнитными сигнатурами. Калиевые изменения, расположенные в центре, характеризуются вторичным биотитом и калиевым полевым шпатом. Они переходят наружу в филлитовый ореол, характеризующийся всепроникающей серицитизацией и пониженным содержанием магнетита. Периферийная пропилитовая зона демонстрирует обильные хлоритовые, эпидотовые, карбонатные минералы и повышенную магнитную восприимчивость из-за сохранности магнетита. Ключевым результатом стало выявление зон, богатых хлоритом и эпидотом, которые, как известно, отрицательно влияют на показатели извлечения флотации, тем самым влияя на эффективность переработки руды. Программное обеспечение Leapfrog Geo облегчило 3D-моделирование, улучшив визуализацию и структурную интерпретацию доменов изменений. Эта комплексная характеристика значительно улучшает геологическое понимание и поддерживает оптимизированные стратегии разведки и переработки, демонстрируя передовой опыт применения современных спектроскопических и геофизических методов к порфировым медным месторождениям.

Ключевые слова: месторождение Бозшаколь, медно-порфировые системы, гидротермальные изменения, минеральная зональность, калиевые изменения, филлитовые изменения, пропилитовые изменения, инфракрасная спектроскопия.

Article submission date: 20.05.2025